UNIVERSITÉ DE GENÈVE

Archive ouverte UNIGE
https://archive-ouverte.unige.ch

Article scientifique | Article | 2024

Published version | Public access

This is the published version of the publication, made available in accordance with the publisher's policy.

Impact of inorganic mercury on carotenoids in freshwater algae: Insights from single-cell resonance Raman spectroscopy

Nesterovschi, Ion; Maškarić, Karlo; Poplăcean, Iuliana-Cornelia; Santos, João; Kantarciyan, Arin; Slaveykova, Vera; Pînzaru, Simona Cîntă

How to cite

NESTEROVSCHI, Ion et al. Impact of inorganic mercury on carotenoids in freshwater algae: Insights from single-cell resonance Raman spectroscopy. In: Aquatic toxicology, 2024, vol. 276, p. 107085. doi: 10.1016/j.aquatox.2024.107085

This publication URL: https://archive-ouverte.unige.ch/unige:180044
Publication DOI: 10.1016/j.aquatox.2024.107085

© The author(s). This work is licensed under a Creative Commons Attribution (CC BY 4.0)
https://creativecommons.org/licenses/by/4.0

Last update in Archive ouverte UNIGE on 18.09.2024 13:15

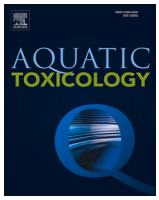
Aquatic Toxicology 276 (2024) 107085



Contents lists available at ScienceDirect

Aquatic Toxicology

journal homepage: www.elsevier.com/locate/aqtox



Impact of inorganic mercury on carotenoids in freshwater algae: Insights from single-cell resonance Raman spectroscopy

Ion Nesterovschi [a,b], Karlo Maškarić [a,b], Iuliana-Cornelia Poplăcean [a], João P. Santos [c], Arin Kantarciyan [c], Vera I. Slaveykova [c,*], Simona Cîntă Pînzaru [a,b,*]

[a] Biomolecular Physics Department, Babeş–Bolyai University, Kogălniceanu 1, RO, 400084, Cluj-Napoca, Romania
[b] Institute for Research, Development and Innovation in Applied Natural Sciences, Babes-Bolyai University, Fantanele 30, Cluj-Napoca, Romania
[c] Environmental Biogeochemistry and Ecotoxicology, Department F.A. Forel for Environmental and Aquatic Sciences, Faculty of Sciences, University of Geneva, 66 Bvd Carl-Vogt 66, CH, 1211, Geneva, Switzerland

ARTICLE INFO

Keywords:
Chlamydomonas reinhardtii
Cyclotella meneghiniana
Resonance Raman spectroscopy
Environmental stress
Heavy metals
Mercury

ABSTRACT

The influence of inorganic mercury (Hg(II)) exposure on photosynthetic microorganisms and their pigments remains understudied. Here, we employed resonance Raman (RR) spectroscopy to investigate the responses of two freshwater phytoplankton species, the green alga *Chlamydomonas reinhardtii* and the diatom *Cyclotella meneghiniana* to Hg(II) exposure. We selectively recorded the spectral RR signature of carotenoids in intact cells exposed to concentrations of 10 nM and 100 nM of Hg(II), representative for contaminated environment and unexposed control cells. A two-hour exposure of *C. reinhardtii* resulted in a slight decrease in lutein and β-carotene levels, while total carotenoids RR band broadening, as revealed by the FWHM of the υ_1(C=C) stretching mode from averaged RR spectra, suggested conformational changes in pigments. Higher Hg(II) concentration induced more pronounced conformational changes. Similarly, a two-hour exposure of *C. meneghiniana* resulted in slight decreased level of the fucoxanthin, while diadinoxanthin showed an opposite trend compared to control: when fucoxanthin decreased, diadinoxanthin increased under 10 nM Hg (II) exposure. At higher concentrations, the decrease in fucoxanthin was less pronounced, accompanied by a broadening of the band area, (with FHHM increased), indicating possible conformer occurrence in response to Hg-induced stress. The changes in the main carotenoid species of the two algae are species-specific, Hg(II) concentration-specific, and dependent on exposure time. The calculated spectral differences in absorbances from UV–VIS spectra of methanol extracts from each group supported the main findings obtained by RR, though with caution due to the selective extraction efficiency of the respective carotenoids. This study highlighted for a first time the capability of single-cell RR spectroscopy as a valuable tool for toxicity assessment and for comprehending early-stage alterations in carotenoid metabolism due to toxic metal exposure in vivo.

1. Introduction

The significant increase of the environmental concentration of mercury (Hg), as a results of the anthropogenic activity, poses a significant threat in aquatic ecosystems (Branfireun et al., 2020; Driscoll et al., 2013). The toxicity responses and tolerance mechanisms of phytoplankton to toxic metal stress, including mercury, as well as underlaying processes have been recently reviewed (Chakravorty et al., 2023; Xiao et al., 2023). For the specific case of mercury, various adverse effects have been reported in algae exposed to high concentrations of inorganic mercury (Hg(II)), including growth rate inhibition, generation of reactive oxygen species (ROS), influence on plasma membrane permeability, chlorophyll degradation etc. (Beauvais-Flück et al., 2018; Le Faucheur et al., 2014). More recent omics studies have revealed a much broader impact of Hg(II) on algal metabolism (Beauvais-Flück et al., 2018; Huang et al., 2022; Slaveykova et al., 2021). For example, an RNA Seq transcriptomics study has shown demonstrated that exposing the green alga *Chlamydomonas reinhardtii* to Hg(II) concentrations ranging from 0.1 nM to 10 nM led to the dysregulation of genes involved in cellular processes, energy metabolism, photosystems, and RedOx homeostasis, consistent with the anticipated toxic effects. In addition, genes involved in cell motility, nutrition, and amino acids metabolism

* Corresponding authors.
E-mail addresses: vera.slaveykova@unige.ch (V.I. Slaveykova), simona.pinzaru@ubbcluj.ro (S.C. Pînzaru).

https://doi.org/10.1016/j.aquatox.2024.107085
Received 26 May 2024; Received in revised form 4 September 2024; Accepted 4 September 2024
Available online 6 September 2024
0166-445X/© 2024 The Authors. Published by Elsevier B.V. This is an open access article under the CC BY license (http://creativecommons.org/licenses/by/4.0/).

were also dysregulated during exposure to low environmental concentrations (Beauvais-Flück et al., 2017). These observations have been further confirmed by metabolomics, revealing alterations in amino acids and nucleotide metabolism, photorespiration and the tricarboxylic acid (TCA) cycle, as well as changes in the metabolism of fatty acids, carbohydrates, and antioxidants in green alga *C. reinhardtii* (Slaveykova et al., 2021). Using integrated omics analyses, a significant upregulation of transcripts and metabolites involved in amino acid synthesis, cellular responses to chemical stress, reactive oxygen species detoxification, and electron transport on other phytoplankton species *Euglena gracilis* exposed to Hg(II) has been reported (Huang et al., 2022). Finally, very recent study has demonstrated that the exposure to Hg(II) resulted in reprogramming of the metabolism of diatom *Cyclotella meneghiniana*, namely induced shifts in amino acids, nucleotides, fatty acids, TCA and antioxidants metabolism in concentration-dependent way (Santos et al., 2024).

Carotenoids are recognized to play an important role in the algal defence against the stress, including exposure to toxic metals, such as mercury (Xiao et al., 2023). They play a protective role for the photosynthetic apparatus of algae against oxidative damage (Lohr, 2023). Total carotenoids contents in various phytoplankton species exposed to Hg(II) are often assessed as biomarkers with reported increase, decrease and no effect on their concentrations. For example, a six-day exposure to 0.45 nM Hg (II) resulted in a slight increase in the total carotenoid content of *Nannochloropsis oculata* compared to the unexposed controls (Zamani-Ahmadmahmoodi et al., 2020). In the microalga *Rhodomonas lens*, total carotenoid concentrations increased after exposure to 5 nM Hg for 48h However, concentrations decreased significantly when Hg exposure concentrations were increased to 1.25 and 2.5 nM (Pinto et al., 2023). Cyanobacterium *Microcystis aeruginosa* exhibited a decrease in total carotenoid concentrations when exposed to increasing concentrations from 5 to 0.15 nM over 96 h with a more pronounced decrease at higher concentrations of 100 and 150 nM, and dependent on exposure time (Pinto et al., 2023). In diatom *Phaeodactylum tricornutum* concentrations of β-carotene, fucoxanthin, diadinoxanthin and diatoxantin were significantly reduced in response to 0.5 nM Hg (II) exposure (Cabrita et al., 2018). However, measuring carotenoid content in most cases relies on invasive methods, which involve cell destruction and extraction in solvents (Saini and Keum, 2018), with efficiency dependence on many factors. Therefore, conclusions are typically drawn exclusively from extracted cells under specific circumstances, which may not reflect their *in vivo* status.

The advances in Raman technology combined with resonance Raman (RR) under appropriate laser excitation, open novel opportunity for non-invasive, selective, and sensitive measurements of the cellular carotenoids without extraction needed (Barletta et al., 2015). Particularly, the resonance Raman spectroscopy, which utilizes laser excitation within the absorption bands of specific molecules, in our case, carotenoids, offers the advantage of selective detection and characterization of these pigments within the whole cell (Nekvapil et al., 2021, 2019). Nevertheless, very few studies have used Raman spectroscopy to explore the effect of different stressors on aquatic biota (Chen et al., 2022; Nekvapil et al., 2021). For example, one similar study showed a red-shift and broadening of the carotenoid Raman band assigned to C=C stretching mode in cyanobacterium *Coelomoron pusillum* facing Zn-ferrite nanoparticles, indicating a change of carotenoid profile towards the increased amount of β-carotene as a stress response (Nekvapil et al., 2021). Another study investigating the effect of salinity stress on carotenoids in *C. reinhardtii* demonstrated that the Raman analysis of the main carotenoid band $\nu_{(C=C)}$ mode indicates an increase of the carotenoids with lower conjugation length (lutein and zeaxanthin) compared to β-carotene, as the function of culture age and salinity stress, which resulted in increased band profile change in total carotenoids, explained by conformational changes induced by salinity stress (Pandey et al., 2022).

Resonance Raman studies of microalgae *C. reinhardtii* and *C. menenghiniana* so far are scant (Alexandre et al., 2014; Pandey et al., 2022). For *C. reinhardtii*, the RR spectra have been used to investigate the changes carotenoids profile under salinity stress (Pandey et al., 2022), but this study showed that both types of photosynthetic pigments, carotenoids and chlorophylls could be detected simultaneously within the same resonance Raman spectrum or carotenoids. The carotenoids species identified were lutein and β-carotene. Interestingly, the study assigned the RR band at 1280 cm^{-1} to chlorophyll, however we argue that under 532 nm excitation, except the three main RR bands of carotenoids, υ_1(C=C), υ_2(C—C) and the υ_3(C—CH_3), other carotenoid bands of weaker intensity, generally observed from photosynthetic organisms, are also present in RR spectra, including that at about 1280 cm^{-1}, according to previous resonance Raman studies of the individual carotenoid molecules (Barletta et al., 2015). Rather non-resonance conditions for both types of pigments, such as those under near-infrared excitation (785 nm) would be more feasible for considering photosynthetic pigments within one single NIR-Raman spectrum. Regarding *C. menenghiniana*, a previous RR study highlighted the possibility to selectively detect in intact cell the main xantophylls: fucoxanthin, diadinoxanthin and diatoxanthin, according to their specific band position in the mixture such as cell (Alexandre et al., 2014).

This study aims to investigate the alteration of carotenoid profiles in vivo using single-cell Raman spectroscopy and to assess the potential of this technique for monitoring changes in these important pigments within phytoplankton cells affected by Hg(II). The spectral signatures associated with Hg (II)-induced stress in green alga *C. reinhardtii* and diatom *C. meneghiniana* are explored by using the resonance and non-resonance Raman spectra at the single-cell level, for statistically relevant number of cells. We hypothesize that exposure to mercury will result in species-specific alterations in carotenoid profiles, with the magnitude and nature of these changes correlating with the concentration of mercury. Green alga *C. reinhardtii* and the diatom *C. meneghiniana* were selected as representing common and abundant classes of freshwater phytoplankton. Photosynthetic microorganisms, as primary producers, hold a crucial position in numerous biogeochemical cycles, sustaining aquatic ecosystems and their services (Falkowski, 1994; Litchman et al., 2015).

2. Materials and methods

2.1. Cell cultures and exposure to Hg(II)

Green alga *Chlamydomonas reinhardtii* (CPCC11, Canadian Phycological Culture Centre, Waterloo, Canada) and *Cyclotella meneghiniana* (CCAC 0036 strain, Collection of Algal Cultures, University of Duisburg-Essen, Germany) were grown axenically in a 4 × diluted Tris-Acetate-Phosphate media (TAP) and a synthetic freshwater media (SFM), respectively (Table S1 in the Appendix).

Cultures were produced in a specialized incubator (Fitotron SGC 120, model SGC120, Weiss Technik UK Ltd., Loughborough, UK) at 20 °C, with a 16/8-h light/dark cycle (100 μmol s^{-1} m^{-2}) and the continuous air supply (~150 mL min^{-1}) filtered through a capsule filter (0.2 μm Aervent®) and two gold-coated quartz sand traps (MERX-T gold trap, Brooks), to prevent any possible contamination. The cells were harvested in their exponential growth phase by gentle centrifugation (TX-1000 ThermoFisher X Pro Series, 15 min, 1346 × *g*, 20 °C), rinsed with and re-suspend in their exposure media (Table S1) to a final density of 1.0×10^6 cell mL^{-1}. The exposure media were supplemented with 10 and 100 nM of inorganic Hg(II) Brooks Rand Instruments (Seattle, WA, USA). The selected concentrations are representative for highly contaminated aquatic environment and correspond to our previous transcriptomics and metabolomics studies (Beauvais-Flück et al., 2018; Santos et al., 2024; Slaveykova et al., 2021).

At the end of the exposure period of 2 h, the cells were centrifuged (6 min, 4062 × *g*, 4 °C), rinsed with Hg-free exposure media. Exposure time of 2 h was selected as it corresponds to the attainment of the steady state

in the uptake kinetics of Hg for *C. reinhardtii* (Beauvais-Flück et al., 2017, Li et al., 2020) and for *C. menegniana* (Santos et al. 2024), with a minimal cellular transformations of Hg(II). In addition, at 2 h exposure no growth inhibition was observed, however the metabolism of both algae was reprogrammed as revealed by metabolomics studies for *C. reinhardii* (Slaveykova et al. 2021) and for *C. meneghiniana* (Santos et al. 2024). The effect of the exposure duration was further tested at 24 h for diatoms to get an insight on the dynamics of the carotenoid's response to Hg(II). Unexposed green algae and diatoms were used as negative controls (NC). All the experiments were performed in 3 independent biological replicates.

2.2. Single-cell Raman spectroscopy

Resonance and non-resonance Raman spectra at single-cell level have been recorded using a Renishaw InVia Raman system with a Leica research grade microscope. For excitation a diode pumped solid state (DPSS) laser, air cooled, emitting at 532 nm line has been employed. The resonance Raman (RR) spectra were measured in the 50–1830 cm^{-1} range with a spectral resolution of 0.5 cm^{-1} and a spatial resolution below 1 μm (lateral, xy) and 1 μm (depth, z). The NIR Raman spectra were recorded in the 712–1830 cm^{-1} range, using a laser diode emitting at 785 nm, for NIR Raman spectral resolution was 1 cm^{-1}. Although the fresh cells exhibited reasonable spectra with acceptable signal-to-noise for short acquisition (to avoid cells heating), the fixed cells revealed strong fluorescence only for 785 nm excitation, regardless the exposure time (tested between 1 and 60 s), the applied laser power (tested between 2 mW and 150 mW) and the number of acquisitions (tested between 1 and 60). Signal detection was achieved with a RenCam CCD detector, 1024 × 256 pixels (200–1060 nm).

The cells were focused using the "coffee ring" resulted from the drop-coating deposition Raman of 1 μL sample of cells batch on a hydrophobic (μ-RIM™ from BioTools) slide, using progressively the 5 × (NA 0.12 WD 13.2 mm), 20 × (NA 0.35, WD 2 mm), 50 × (NA 0.75, WD 0.37 mm) and 100 × (NA 0.9, WD 3.4 mm) microscope objectives. The optical micrographs of the cells were collected with the Raman microscope assisted by Renishaw camera. Data acquisition has been achieved using the Wire 3.4 software by optimizing condition and setting 1 s exposure, 1 accumulation and 1 % laser power (2 mW).

2.3. UV–Vis measurement

Both unexposed control and exposed to inorganic Hg(II) at 10 nM and 100 nM during 2 h and 24 h cultures of *C. meneghiniana* and *C. reinhardtii* were investigated by recording the absorbance spectra in the range 300 to 800 nm with a scan step of 1 nm using Microplate reader (Synergy H1 Hybrid, BioTek, Germany). The absorbance spectra of cell cultures were recorded before and after methanol extraction. For pigment extraction, 5 mL of cell aliquot was collected and washed with clean exposure media before resuspension in 1 mL of pure methanol (Merck, Germany). Once in methanol, cells were sonicated for 1 min in ice (Branson Ultrasonics™) and kept in dark overnight at 4 °C. The extracts were then centrifuged at 4062 × *g* for 10 min and the supernatants were sampled for spectral absorbance scanning.

2.4. Computational processing

The processing operation for resonance Raman spectra of cells involved several steps using Python 3.11 programming language. Initially, noise reduction was performed using Wiener filter technique, followed by baseline subtraction employing Improved Asymmetric Least Squares algorithm. Subsequently, two distinct methodologies were applied for analysis. The first approach consisted in the deconvolution of the C=C Raman mode from the average spectrum calculated from 150 independent raw spectra from each group, while the second approach employed the deconvolution of individual band from each raw Raman spectrum from distinct cells. Within the second approach, the data were subsequently clustered using the KMeans algorithm. For the average spectra acquired from each exposure case (in total 9 averaged Raman spectra), deconvolution was conducted specifically targeting the υ_1(C=C) stretching mode band using a Lorentzian function. The number of band components for deconvolution was iteratively determined based on optimizing the R^2-score.

In the second method, each spectrum was individually subjected to deconvolution, and the resulting peak characteristics (including intensity, FWHM, and area) were extracted. These characteristics were then clustered using the KMeans algorithm with the Silhouette score used to determine the optimal number of clusters. This approach was incorporated for statistical analysis.

3. Results

3.1. Characterization of algae exposed to Hg with single-cell RR spectroscopy

RR spectra of the two photosynthetic species non-exposed to Hg(II) exhibited typical spectral features showing at least 10 distinct bands in the 900–1600 cm^{-1}, spectral range, where the dominant ones are the three main vibrational modes assigned to the skeletal molecular structure of carotenoids (Fig. S1). The weak bands observed in the RR spectra are also assigned to their specific carotenoids. In our opinion, the chlorophyll Raman bands are not observed in the resonance Raman spectra of carotenoids excited with 532 nm.

To explore the effect of Hg(II) exposure on green algae and diatom, overall of 1350 Raman spectra were collected, with 150 spectra obtained for each group of treatment, both controls and exposed to 2 values of Hg(II) concentrations. Spectral data recorded and processed from each case of exposure were considered by calculating the averaged spectrum corresponding for each treatment. Thus, it resulted nine averaged spectra, three corresponding for *C. reinhardtii* (control – NC, exposed to 10 nM Hg(II) and exposed to 100 nM Hg(II)), three for *C. menenghiniana* exposed for 2 h, and three for *C. menenghiniana* for 24 h exposure (Fig. 1). All the resonance Raman spectra of both exposed and unexposed cells exhibited prominent bands at 1521 – 1524 cm^{-1} (ν_1(C = C)), 1154–1157 cm^{-1} (ν_2(C—C)) and at 1003–1009 cm^{-1} (ν_3(C—CH_3)) among other minor bands, all of them correspond to the resonance Raman spectra of the carotenoids (Alexandre et al., 2014; Pandey et al., 2022). Details of the spectral range from 1460 – 1560 cm^{-1}, where the C=C bond of the carotenoids is recorded, are shown in the Fig. 2, the right panel. Here, the deconvolution in two main components is displayed for each case. The two Lorentzian deconvoluted components (R^2 = 0.998) peaked at 1517 and 1524 cm^{-1} for *C. reinhardtii* and at 1521 and 1530 cm^{-1} for *C. menenghiana*, respectively, were further analyzed regarding their change upon Hg(II) exposure. Note, the two Lorentzian components peaked at the same position in both exposed and control treatments, however their relative intensity, thus their individual contribution to the overall band envelope is slightly changed, therefore the two components were carefully investigated by calculating intensity, FWHM and area for each treatment. The calculated values are summarized in Table S2, while the comparative plotted values are summarized in the Fig. 2.

These changes may be attributed to the variation of existing carotenoids concentration, emergence of new carotenoids, isomeric or conformational transformations in existing carotenoids, reflected in changes of the band profile, intensity, FWHM, and total band area. To ascertain the most plausible explanation, we conducted a deconvolution of the Raman spectra in the range 1480 – 1560 cm^{-1} range, comprising this band. Two approaches were employed for the analysis, firstly, deconvolution of the average spectrum and secondly, the deconvolution of each individual Raman spectrum from each cell followed by clustering of the results.

First, approach offered a rapid solution but potentially prone to

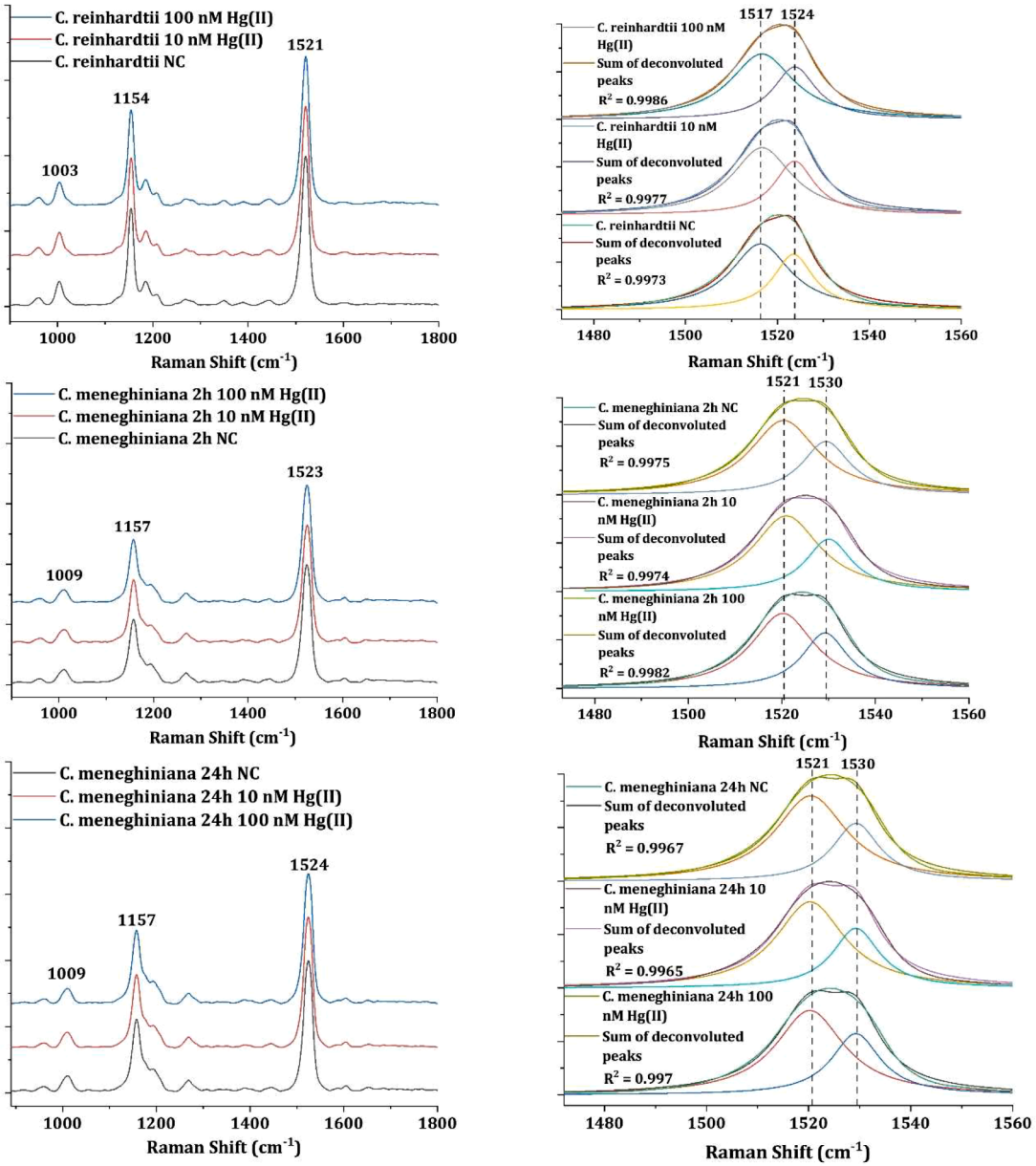


Fig. 1. The average resonance Raman spectra for *C. reinhardtii* and *C. meneghiniana* in the absence (NC-negative control) and presence of 10 and 100 nM of Hg(II). Exposure time: 2 h and 24 h Detailed zoom in the main C=C band is shown on the right panel, along with the deconvoluted components, as indicated.

artifacts due to variations in the number of identifiable carotenoids among spectra, since many carotenoids' species exhibit C=C Raman band at about 1520 – 1526 cm^{-1} range, being sensitive to their local environmental conditions. Second approach, which used the deconvolution of each individual Raman spectrum, followed by clustering of the results apparently worked more favourable but required higher time load and another drawback is the processing of spectral output from all the cells including those underdeveloped or potentially destroyed during sample processing. Both approaches consistently revealed the presence of two main components of the C=C band which are tentatively assigned to the most abundant carotenoids species specific for *C. reinhardtii* (lutein and β-carotene) (Pandey et al., 2022) and *C. menenghiniana* (fucoxanthin and diadinoxanthin) (et al., 2014b), respectively. Other minor contributions to the overall band from other carotenoids species, although present, were not considered in comparative analyses. The result is consistent with a previous resonance Raman study, which identified for *C. reinhardtii* two main carotenoids, β-carotene and lutein, exhibiting resonance Raman spectra with identified band components at 1517 and 1524 cm^{-1} (Pandey et al., 2022). The carotenoids corresponding to the given positions were identified based on the previous reports (Alexandre et al., 2014; Andreeva and Velitchkova, 2005; Ballard et al., 1989; Kish et al., 2015; Llansola-Portoles et al., 2017; Macernis et al., 2022, 2014; Nekvapil et al., 2022; Pinto et al., 2021; Uragami et al., 2018) comprising both Raman and HPLC techniques (Akepach et al., 2022; Chukhutsina et al., 2014; Cordero et al., 2011; Huang et al., 2023; Rathod et al., 2020; Veith et al., 2009). From the RR studies, the number of double bonds and functional groups such as -OH were taken into consideration. Thus, a smaller number of conjugated double bonds in the carotenoid skeletal structure (as in the case of lutein) would result in the position of the C=C band at a higher wavenumber, while the additional functional groups would give a right-shift of the band position (Kish et al., 2015; Llansola-Portoles et al., 2017; Macernis et al., 2014; Uragami et al., 2018). The existent HPLC studies (Akepach et al., 2022; Chukhutsina et al., 2014; Cordero et al., 2011; Huang et al., 2023; Rathod et al., 2020; Veith et al., 2009), which analyzed carotenoids by identifying and calculating their

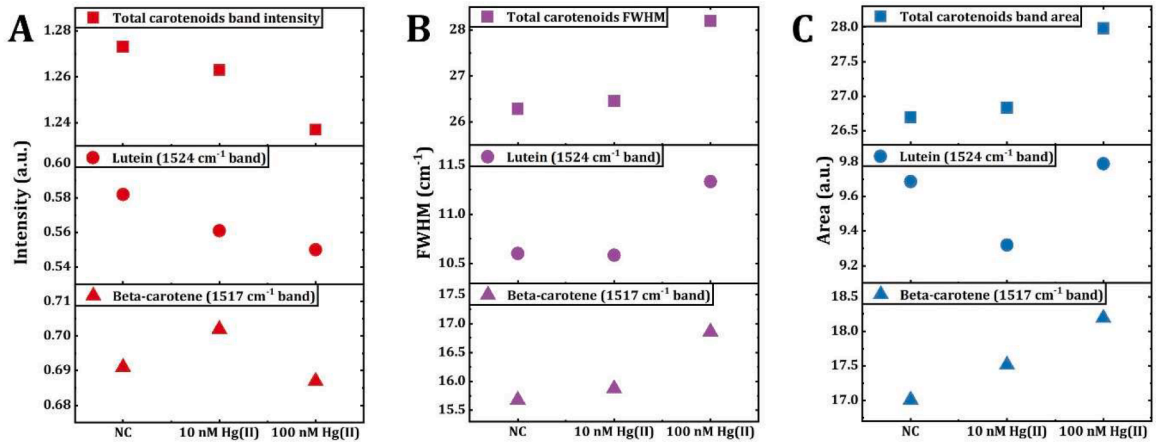


Fig. 2. The intensity (A), FWHM (B) and the area (C) of the bands found by deconvolution of the C=C mode from RR spectra in *C. reinhardtii* negative control (NC) and exposed to 10 and 100 nM Hg(II).

concentrations, served for validation of the identified carotenoids in our study. This validation is achieved by correlating the intensities of Raman bands observed in our study with the concentrations identified through high-precision liquid chromatography studies mentioned above. As highlighted in the Fig. 2, a slight decrease the band intensity of lutein was observed at 10 nM exposure, while with increasing Hg(II) concentration to 100 nM, the decreased tendency is accompanied by lutein band broadening indicating its conformational changes. Additionally, the band broadening (Fig. 2B, FWHM increases) is observed with increasing Hg concentration. β-carotene level clearly increased at 10 nM exposure, and further a decreased tendency and band broadening was observed, suggesting rapid and complex conformational changes of this carotenoid with increasing stressor level. Overall, the total carotenoids band area is increased while the individual components lutein and beta-carotene suffered different tendencies (Fig. 2C) with lutein first decreasing for 10 nM and then decreasing with a lower extent for 100 nM, while beta-carotene is clearly increased with increasing Hg(II) concentration. However, using the second methodological approach for data processing, the carotenoid changes trend is likely similar with that from the first approach, but the observed differences are more subtle (Fig. S4).

The band area being a mathematically calculated parameter as the product of the intensity and FWHM, follows a trend which, hypothetically could suggest the decrease in the concentration of the carotenoids, with increasing concentration of Hg(II) but the increasing the FWHM with Hg(II) exposure strongly suggest that other carotenoids or different isomers or different conformations of them occur as a complex molecular response to stress.

For *C. meneghiniana*, two main carotenoids – diadinoxanthin at 1521 cm^{-1} and fucoxanthin at 1530 cm^{-1} – were identified (Fig. 3) (Alexandre et al., 2014; Ikeda et al., 2008; Nekvapil et al., 2022; Veith et al., 2009) using similar protocol of identification as in the case of *C. reinhardtii*. The detailed spectral band analyses of exposed cells compared to the negative control (NC) are presented in the Fig. 3, while the corresponding plotted values are summarized in Tables S2 – S5. Results from 2 h exposure to Hg(II) indicated a decrease in the intensity and an increase in FHWM and band area similar to the case for *C. reinhardtii*. However, each identified carotenoids responded differently to Hg(II) exposure. These differences were notable at 10 nM of Hg(II), where fucoxanthin exhibited the lowest level, which then increased at 100 nM of Hg(II). Diadinoxanthin firstly increased (band intensity and area increased), then decreased rapidly with increasing Hg concentration. It appears that the two main carotenoids, fucoxanthin and diadinoxanthin exhibited contrasting trends. When fucoxanthin decreased under exposure to 10 nM of Hg (II) compared to the control, diadinoxanthin is increased. However, at higher concentrations, the decrease in fucoxanthin was less pronounced, with a broader band area, (indicated by increased FHHM) suggesting the possible occurrence of conformers in response to stress. Clearly, the alterations in the main carotenoid species of the two algae do not exhibit a linear relationship with the concentration of Hg.

The results for 24 h exposure to Hg(II) (Fig. 4) revealed a slightly different picture compared with that recorded for 2 h exposure.

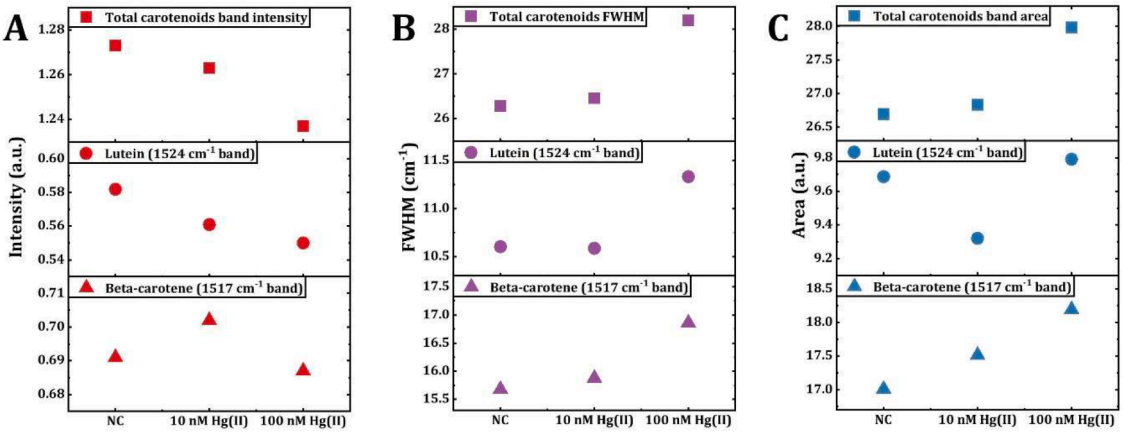


Fig. 3. The intensity (A), FWHM (B) and the area (C) of the bands found by deconvolution of the C=C mode from RR spectra of *C. meneghiniana* negative control (NC) and exposed to 10 and 100 nM Hg(II) for 2 h

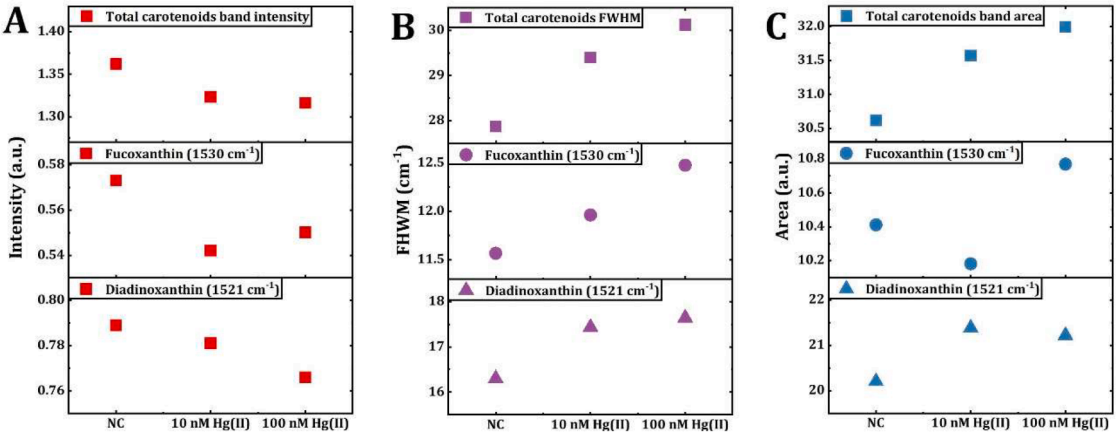


Fig. 4. The intensity (A), FWHM (B) and the area (C) of the bands found by deconvolution of the C=C mode from RR spectra of *C. meneghiniana* negative control (NC) and exposed to 10 and 100 nM Hg(II) for 24 h.

Decreasing total carotenoid intensity and increasing FHWM (band broadening) and band area were clearly observed. Also, the main identified carotenoids responded similarly, with clear decreased in fucoxanthin level at 10 nM Hg(II) comparative to control. At higher Hg concentration, fucoxanthin level also decreased (band intensity decreased) compared to control, but to a lower extent than at lower Hg concentration, accompanied by band broadening (FWHM increased) and total band area increased, suggesting drastic conformational change (Fig. 4A-C). It appears that longer exposure (24 h) induced other conformational changes in carotenoids profile, thus, we can assume that such subtle molecular changes are concentration - specific and exposure time - dependent. Summarizing, 24 h exposure to Hg(II) resulted in decreased concentration of all-trans fucoxanthin and diadinoxanthin compared to negative control along with the occurrence of new conformers (total carotenoids band area increasing, band broadening (Fig. 4B and C). Certainly, carotenoids bands parameters change undergoes different trend for different exposure time.

Using the clustering methodological approach for data processing (Figs. S4 – S6), the Raman band characteristics of the carotenoids changed similarly to the first approach, but the differences are less pronounced. Considering the two computational approaches and the interpretability of the results, it appeared advantageous to compare their performance and select the one that best highlights such subtle changes in intact cells.

3.2. Characterization of the algae using UV–Vis spectrophotometry

The raw UV–Vis spectra recorded on algal extract (Fig. S3) revealed slight decrease in the absorbance levels of the whole spectrum of extracts from exposed cells, but the differences are difficult to be observed, therefore we applied the calculation of the spectral differences between absorbance spectra of the extracts from the exposed cells and negative control. These differences for each treatment are displayed in the Fig. 5A. In the case of *C. reinhardtii*, the spectral differences revealed prominent peaks at 437 and 470 nm highlighting the existent differences in carotenoid content of exposed cells (10 nM Hg(II)) to control, although they are very small (0.04 counts in absorbance difference). For the 100 nM Hg(II) exposure these differences are visible in the peaks at 435 and 468 nm, slightly shifted to lower wavelength from those for 10 nM Hg(II) exposure, suggesting slightly different carotenoid conformation. Finally, calculated spectral absorbance difference between cells under 10 and 100 nM Hg(II) exposure clearly indicate more prominent change in carotenoids conformation (differences peaked at 434 and 467 nm).

In the case of *C. menenghiana* UV–Vis absorbance differences (Fig. 5B and C), showed different shape, however there are in negative range

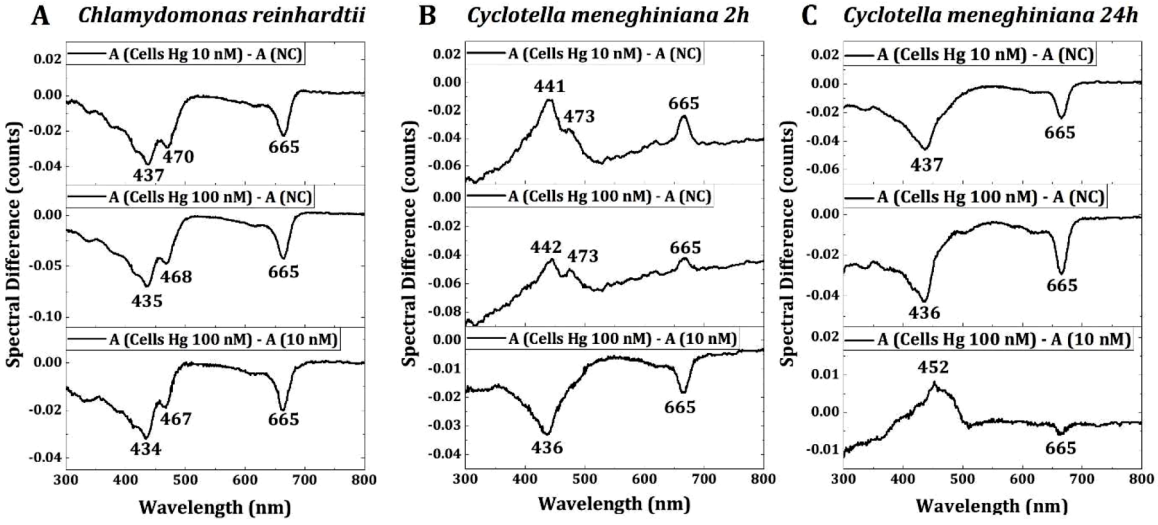


Fig. 5. Spectral difference between UV–Vis spectra of different concentrations of mercury exposure, of the methanol extracts of green alga *C reinhardtii* at 2 h exposure (A) and diatom *C. meneghiniana* at 2 h (B) and 24 h (C) exposure to 10 and 100 nM of Hg(II). NC denotes negative control of unexposed algae.

highlighting change in carotenoids peaked at 441 and 473 nm, between extracts exposed to 10 nM Hg(II) versus control. The differences are increasing within increasing concentration of mercury exposure (peaked at 442 and 473 nm). However, this consideration should be regarded with caution, considering the spectral resolution of 1 nm. Peaks deviation with 1–2 nm could however suggest changes in the electronic transitions according to the modified electronic structure of given carotenoid species due to its conformational change. Absorbance differences between extracts of cells under different concentrations of Hg exposure clearly highlighted the peak at 436 nm, indicating conformational change in carotenoids profile. Finally, *C. menenghiana* exposed for 24 h showed absorbances extracts clearly different from those exposed to 2 h (Fig. 5C). In this case the spectral differences peaked at 436 nm, for 10 nM exposure and 437 nm for 100 nM exposure, while the differences between level of exposure results in a clear different peak 452 nm, which perfectly corresponds with the absorbance of fucoxanthin in methanol. Comparing the data from the two photosynthetic species their spectral response in terms of absorbance is clearly different and supports the main findings from the RR analyses.

Considering the decrease of chlorophyll absorbance across all exposed cases, the chlorophyll peak was consistently observed at 665 nm with absorbance spectral differences falling within the range of 0.02 – 0.03 arbitrary units. The overall UV–Vis data revealed subtle differences between different level of exposure and control. In the NIR-Raman data obtained using 785 nm excitation of fixed cells, both control and Hg (II)-exposed exhibited strong fluorescence only. Therefore, considerations regarding chlorophylls levels from NIR-Raman data were not utilized.

The spectral calculations derived from UV–Vis spectra support and validate the findings described from analysis of resonance Raman spectra. Linear correlation between Raman and UV–Vis data is not expected, given that Raman read-out pertains to the entire intact cells, while UV–Vis data addresses the resulting extracts in methanol, which may not efficiently recover all carotenoid species. It's worth noting that due to its non-polar nature, β-carotene cannot be effectively extracted using polar solvents like methanol. Hence, the results of UV–Vis analysis of the extracts actually describe the most extractable carotenoids in methanol in the given extraction conditions.

4. Discussion

The results of the present study clearly indicate that the exposure to Hg(II) alters the concentrations and conformations of main carotenoids in the studies algae in both time- and concentration- dependent manner. This general conclusion is also supported by the decreased UV–Vis spectral absorbance and the intensity of identified carotenoids Raman bands in correlation with Hg(II) exposure. These experimental observations can be explained by changes in biosynthesis cycle of carotenoids (Beauvais-Flück et al., 2018; Santos et al., 2024; Slaveykova et al., 2021), and their complex molecular involvement in the photosystem complexes. To get insight into these processes, however alternative techniques would bring additional insights, such as the time-resolved spectroscopy (from femtoseconds to microseconds) to obtain information on the relaxation and excitation energy-transfer pathways of carotenoids in photosynthetic pigment-protein complex under Hg(II) stress. The advantage of the present approach relies on the comprehensive view of the carotenoids undergoing changes within intact photosynthetic cells under Hg(II) stress, thus, difficult to validate with a conventional approach, since no other technique can provide the same information without employing a procedure for extraction of carotenoids. Therefore, validating with UV–Vis (or others) can be considered to a certain extent, having in mind the specificity of every preparation protocol with specific advantages and limitations.

The biosynthesis of carotenoids and other isoprenoids in *C. reinhardtii* starts with the formation of the active isoprene from the Calvin-Benson cycle intermediated by pyruvate and glyceraldehyde-3-phosphate succeeded by the MEP pathway (Lohr, 2023). Tentatively, it can be hypothesized that the exposure to Hg(II) led to reprogramming of the pyruvate synthesis. For example, pyruvate can be also produced via catabolism of the glycogenic amino acids, such as alanine, serine, cysteine. In plants, alanine is directly converted to pyruvate by alanine aminotransferases; serine can be deaminated by serine dehydratase activity, cysteine is converted to pyruvate by cysteine desulfhydrase (Hildebrandt et al., 2015; Vallon and Spalding, 2009). A previous metabolomic study (Slaveykova et al., 2021) demonstrated that exposure of *C. reinhardtii* to comparable concentrations of Hg(II) resulted in an increase of the abundance of alanine and serine in comparison to unexposed control. However, for diatom *C. meneghiniana* the exposure to Hg(II) resulted in a decrease in the abundance of serine and no effect on the alanine concentrations (Santos et al., 2024).

The changes in the carotenoid concentrations are also consistent with results on metabolic perturbation in different precursors of carotenoid synthesis in *C. reinhardtii* and *C. meneghiniana* exposed to Hg(II) (Santos et al., 2024; Slaveykova et al., 2021). The phenylalanine and tyrosine, known to be precursors for the synthesis of pigments, including carotenoids and phytochelatins via coumarate and acetoacetyl CoA pathway (Rea et al., 2018), accumulated in both *C. meneghiniana* (Santos et al., 2024) and *C. reinhardtii* (Slaveykova et al., 2021) exposed for 2 h to 10 and 100 nM Hg(II). Similarly lysine is accumulated in both phytoplankton species upon Hg(II) exposure, and its metabolism leads to acetoacetyl CoA that provides precursors for carotenoids and the xanthophyll cycle via the mevalonate pathway (Rea et al., 2018). The interpretation of full width at half maximum observed in RR spectra presents a more intricate scenario. Although studies concerning FWHM variations in organic substances within cells are limited, parallels can be drawn from Raman studies on crystals. In solid, polycrystalline materials such as solid carotenoids, FWHM reflects the level of crystallinity and the co-existence of isomeric forms and their interaction with the local environment or the neighbour molecule (stacked in sandwich-like structures or "head-to-tail" arrangement (Cong et al., 2020; Nesbitt et al., 2018; Yao et al., 2019), with wider bands indicating more conformations and interaction. From here, we can hypothesize that a carotenoid characterized by a wider band possesses higher isomeric diversity in the thylakoid membrane or undergoes multiple conformational changes. Based on the results, with the increase in mercury concentration, there is also a significant positive change (compared to the intensity) of FWHM. Carotenoids band broadening under stress might also suggest changes in the energy transfer chlorophyll-carotenoids within photosystem. The replacement of the magnesium in chlorophyll affects the photon-charge transfer, resulting in the absorption of the photon by the carotenoid, succeeded by his isomerization (Andreeva et al., 2011; Telegina et al., 2023), which is observed by the increasing FWHM.

Overall, this study demonstrated the ability of single-cell resonance Raman spectroscopy (RR) to detect Hg(II)-induced alterations in the primary carotenoids of algae cells in vivo, suggesting their potential use as biomarkers for Hg-induced stress in contaminated environments. However, accurately identifying carotenoids present at lower concentrations remains challenging without additional precise techniques. The variability of resonance Raman spectra in individual carotenoid molecules, influenced by their environmental context, adds further complexity to their identification, which is a limitation of this method. Future research focusing on pollutant concentrations similar to those found in natural environments and longer exposure times, relevant to chronic low-level contamination, could provide further insights into the utility of single-cell RR for assessing the impact of pollutants in aquatic ecosystems.

5. Conclusion

The single-cell resonance Raman spectroscopy revealed for a first time a pronounced perturbation of carotenoid metabolism induced by

exposure to nanomolar concentrations of Hg(II) in intact cells of green alga *C. reinhardtii* and diatom *C. meneghiniana*. These changes were species-specific, yet each carotenoid species responded in a slightly distinct manner. In *C. reinhardtii* exposure to Hg(II) induced slight decrease in lutein, β-carotene levels; total carotenoids showed broadening, indicating pigment conformational changes. In *C. meneghiniana* a decrease in fucoxanthin and an increase in diadinoxanthin under 10 nM Hg(II) treatment were found, while higher concentrations induced less pronounced fucoxanthin decrease. The observed broadening of bands suggested conformer occurrence. This study demonstrates the potential of a single-cell resonance Raman Spectroscopy as a tool for rapid non-invasive toxicity evaluation and for understanding the alterations in the carotenoid's metabolism and their use as specific biomarkers.

Data availability

Processed data are contained within the article. Raw data are available upon request.

Funds

The present study was partially supported by the Swiss National Science Foundation grants 175721.

CRediT authorship contribution statement

Ion Nesterovschi: Writing – original draft, Methodology, Investigation, Formal analysis, Conceptualization. **Karlo Maškarić:** Methodology, Investigation, Formal analysis, Data curation. **Iuliana-Cornelia Poplăcean:** Software, Investigation, Formal analysis. **João P. Santos:** Writing – review & editing, Investigation, Formal analysis. **Arin Kantarciyan:** Writing – original draft, Investigation, Formal analysis. **Vera I. Slaveykova:** Writing – review & editing, Writing – original draft, Validation, Supervision, Project administration, Investigation, Formal analysis, Conceptualization. **Simona Cîntă Pînzaru:** Writing – review & editing, Writing – original draft, Validation, Supervision, Project administration, Investigation, Formal analysis, Conceptualization.

Declaration of competing interest

The authors declare that they have no known competing financial interests or personal relationships that could have appeared to influence the work reported in this paper.

Data availability

Data will be made available on request.

Supplementary materials

Supplementary material associated with this article can be found, in the online version, at doi:10.1016/j.aquatox.2024.107085.

References

Akepach, P., Ribeiro-Filho, N., Wattanakul, J., Darwish, R., Gedi, M.A., Gray, D.A., 2022. Bioaccessibility of carotenoids (β-carotene and lutein) from intact and disrupted microalgae (Chlamydomonas reinhardtii). LWT 160, 113292. https://doi.org/10.1016/J.LWT.2022.113292.

Alexandre, M.T.A., Gundermann, K., Pascal, A.A., Van Grondelle, R., Büchel, C., Robert, B., 2014. Probing the carotenoid content of intact Cyclotella cells by resonance Raman spectroscopy. Photosynth. Res. 119, 273–281. https://doi.org/10.1007/S11120-013-9942-Y.

Andreeva, A., Apostolova, I., Velitchkova, M., 2011. Temperature dependence of resonance Raman spectra of carotenoids. Spectrochim. Acta A Mol. Biomol. Spectrosc. 78, 1261–1265. https://doi.org/10.1016/J.SAA.2010.12.071.

Andreeva, A., Velitchkova, M., 2005. Resonance Raman spectroscopy of carotenoids in Photosystem I particles. Biophys. Chem. 114, 129–135. https://doi.org/10.1016/J.BPC.2004.11.012.

Ballard, L.J., Glasgow, L.A., Hoskins, L.C., Krohe, T., 1989. The resonance Raman excitation profile of fucoxanthin. Spectrochim Acta A 45, 1235–1238. https://doi.org/10.1016/0584-8539(89)80235-1.

Barletta, R.E., Krause, J.W., Goodie, T., El Sabae, H., 2015. The direct measurement of intracellular pigments in phytoplankton using resonance Raman spectroscopy. Mar. Chem. 176, 164–173. https://doi.org/10.1016/J.MARCHEM.2015.09.005.

Beauvais-Flück, R., Slaveykova, V.I., Cosio, C., 2017. Cellular toxicity pathways of inorganic and methyl mercury in the green microalga Chlamydomonas reinhardtii. Sci. Rep. 7 (1), 8034. https://doi.org/10.1038/s41598-017-08515-8.

Beauvais-Flück, R., Slaveykova, V.I., Cosio, C., 2018. Molecular effects of inorganic and methyl mercury in aquatic primary producers: comparing impact to a macrophyte and a green microalga in controlled conditions. Geosciences (Basel) 8. https://doi.org/10.3390/GEOSCIENCES8110393.

Branfireun, B.A., Cosio, C., Poulain, A.J., Riise, G., Bravo, A.G., 2020. Mercury cycling in freshwater systems - An updated conceptual model. Sci. Total Environ. 745, 140906 https://doi.org/10.1016/J.SCITOTENV.2020.140906.

Cabrita, M.T., Duarte, B., Gameiro, C., Godinho, R.M., Caçador, I., 2018. Photochemical features and trace element substituted chlorophylls as early detection biomarkers of metal exposure in the model diatom Phaeodactylum tricornutum. Ecol. Indic. 95, 1038–1052. https://doi.org/10.1016/J.ECOLIND.2017.07.057.

Chakravorty, M., Nanda, M., Bisht, B., Sharma, R., Kumar, S., Mishra, A., Vlaskin, M.S., Chauhan, P.K., Kumar, V., 2023. Heavy metal tolerance in microalgae: detoxification mechanisms and applications. Aquat. Toxicol. 260, 106555 https://doi.org/10.1016/J.AQUATOX.2023.106555.

Chen, K., Wu, X., Zou, Z., Dong, Y., Zhang, S., Li, Xiaofen, Gouda, M., Chu, B., Li, C.M., Li, Xiaoli, He, Y., 2022. Assess heavy metals-induced oxidative stress of microalgae by Electro-Raman combined technique. Anal. Chim. Acta 1208, 339791. https://doi.org/10.1016/J.ACA.2022.339791.

Chukhutsina, V.U., Büchel, C., Van Amerongen, H., 2014. Disentangling two non-photochemical quenching processes in Cyclotella meneghiniana by spectrally-resolved picosecond fluorescence at 77 K. Biochimica et Biophysica Acta (BBA) - Bioenergetics 1837, 899–907. https://doi.org/10.1016/J.BBABIO.2014.02.021.

Cong, X., Liu, X.L., Lin, M.L., Tan, P.H., 2020. Application of Raman spectroscopy to probe fundamental properties of two-dimensional materials. npj 2D Mater. Appl. 4, 1–12. https://doi.org/10.1038/s41699-020-0140-4, 2020 4:1.

Cordero, B.F., Couso, I., León, R., Rodríguez, H., Vargas, M.Á., 2011. Enhancement of carotenoids biosynthesis in Chlamydomonas reinhardtii by nuclear transformation using a phytoene synthase gene isolated from Chlorella zofingiensis. Appl. Microbiol. Biotechnol. 91, 341. https://doi.org/10.1007/S00253-011-3262-Y.

Driscoll, C.T., Mason, R.P., Chan, H.M., Jacob, D.J., Pirrone, N., 2013. Mercury as a global pollutant: sources, pathways, and effects. Environ. Sci. Technol. 47, 4967–4983. https://doi.org/10.1021/ES305071V/ASSET/IMAGES/LARGE/ES-2012-05071V_0004.JPEG.

Falkowski, P.G., 1994. The role of phytoplankton photosynthesis in global biogeochemical cycles. Photosynth. Res. 39, 235–258. https://doi.org/10.1007/BF00014586.

Hildebrandt, T.M., Nunes Nesi, A., Araújo, W.L., Braun, H.P., 2015. Amino acid catabolism in plants. Mol. Plant 8, 1563–1579. https://doi.org/10.1016/J.MOLP.2015.09.005.

Huang, D., Liu, C., Su, M., Zeng, Z., Wang, C., Hu, Z., Lou, S., Li, H., 2023. Enhancement of β-carotene content in Chlamydomonas reinhardtii by expressing bacterium-driven lycopene β-cyclase. Biotechnology for Biofuels and Bioproducts 16, 1–8. https://doi.org/10.1186/S13068-023-02377-1/FIGURES/6.

Huang, H., Mangal, V., Rennie, M.D., Tong, H., Simpson, M.J., Mitchell, C.P.J., 2022. Mercury methylation and methylmercury demethylation in boreal lake sediment with legacy sulphate pollution. Environ Sci Process Impacts 24, 932–944. https://doi.org/10.1039/D2EM00064D.

Ikeda, Y., Komura, M., Watanabe, M., Minami, C., Koike, H., Itoh, S., Kashino, Y., Satoh, K., 2008. Photosystem I complexes associated with fucoxanthin-chlorophyll-binding proteins from a marine centric diatom, Chaetoceros gracilis. Biochimica et Biophysica Acta (BBA) - Bioenergetics 1777, 351–361. https://doi.org/10.1016/J.BBABIO.2008.01.011.

Kish, E., Pinto, M.M.M., Kirilovsky, D., Spezia, R., Robert, B., 2015. Echinenone vibrational properties: from solvents to the orange carotenoid protein. Biochimica et Biophysica Acta (BBA) - Bioenergetics 1847, 1044–1054. https://doi.org/10.1016/J.BBABIO.2015.05.010.

Le Faucheur, S., Campbell, P.G.C., Fortin, C., Slaveykova, V.I., 2014. Interactions between mercury and phytoplankton: speciation, bioavailability, and internal handling. Environ. Toxicol. Chem. 33, 1211–1224. https://doi.org/10.1002/ETC.2424.

Li, M., Liu, W., Slaveykova, V.I., 2020. NanoTiO_2 materials mitigate mercury uptake and effects on green alga Chlamydomonas reinhardtii in mixture exposure. Aq. Tox. 224, 105502. https://doi.org/10.1016/j.aquatox.2020.105502.

Litchman, E., de Tezanos Pinto, P., Edwards, K.F., Klausmeier, C.A., Kremer, C.T., Thomas, M.K., 2015. Global biogeochemical impacts of phytoplankton: a trait-based perspective. J. Ecol. 103, 1384–1396. https://doi.org/10.1111/1365-2745.12438.

Llansola-Portoles, M.J., Pascal, A.A., Robert, B., 2017. Electronic and vibrational properties of carotenoids: from in vitro to in vivo. J. R. Soc. Interface 14. https://doi.org/10.1098/RSIF.2017.0504.

Lohr, M., 2023. Carotenoids in Chlamydomonas. The Chlamydomonas Sourcebook, 2. Organellar and Metabolic Processes, pp. 733–761. https://doi.org/10.1016/B978-0-12-821430-5.00024-9.

Macernis, M., Streckaite, S., Litvin, R., Pascal, A.A., Llansola-Portoles, M.J., Robert, B., Valkunas, L., 2022. Electronic and vibrational properties of allene carotenoids. J. Phys. Chem. A 126, 813–824. https://doi.org/10.1021/ACS.JPCA.1C09393.

Macernis, M., Sulskus, J., Malickaja, S., Robert, B., Valkunas, L., 2014. Resonance Raman spectra and electronic transitions in carotenoids: a density functional theory study. J. Phys. Chem. A 118, 1817–1825. https://doi.org/10.1021/JP406449C.

Nekvapil, F., Brezestean, I., Lazar, G., Firta, C., Pinzaru, S.C., 2022. Resonance Raman and SERRS of fucoxanthin: prospects for carotenoid quantification in live diatom cells. J. Mol. Struct. 1250, 131608 https://doi.org/10.1016/J.MOLSTRUC.2021.131608.

Nekvapil, F., Brezeştean, I., Tomšić, S., Müller, C., Chiş, V., Cintă Pinzaru, S., 2019. Microsphere packages of carotenoids: intact sea urchin eggs tracked by Raman spectroscopy tools. Photochemical and Photobiological Sciences 18, 1933–1944. https://doi.org/10.1039/C9PP00181F/METRICS.

Nekvapil, F., Bunge, A., Barbu Tudoran, L., Cintă Pinzaru, S., 2021. Single-cell Raman micro-spectroscopy for tracking of carotenoids in cyanobacteria exposed to Mn and Zn doped ferrite nanoparticles. Spectrochim. Acta A Mol. Biomol. Spectrosc. 254 https://doi.org/10.1016/J.SAA.2021.119607.

Nesbitt, H.W., Bancroft, G.M., Henderson, G.S., 2018. Temperature dependence of Raman shifts and line widths for Q0 and Q2 crystals of silicates, phosphates, and sulfates. Am. Mineral. 103, 966–976. https://doi.org/10.2138/AM-2018-6314.

Pandey, S., Archana, G., Bagchi, D., 2022. Micro-Raman spectroscopy of the light-harvesting pigments in Chlamydomonas reinhardtii under salinity stress. Spectrochim. Acta A Mol. Biomol. Spectrosc. 281 https://doi.org/10.1016/J.SAA.2022.121613.

Pinto, E.P., Paredes, E., Bellas, J., 2023. Influence of microplastics on the toxicity of chlorpyrifos and mercury on the marine microalgae Rhodomonas lens. Sci. Total Environ. 857, 159605 https://doi.org/10.1016/J.SCITOTENV.2022.159605.

Pinto, R., Vilarinho, R., Carvalho, A.P., Moreira, J.A., Guimarães, L., Oliva-Teles, L., 2021. Raman spectroscopy applied to diatoms (microalgae, Bacillariophyta): prospective use in the environmental diagnosis of freshwater ecosystems. Water Res. 198, 117102 https://doi.org/10.1016/J.WATRES.2021.117102.

Rathod, J.P., Vira, C., Lali, A.M., Prakash, G., 2020. Metabolic engineering of chlamydomonas reinhardtii for enhanced β-carotene and lutein production. Appl. Biochem. Biotechnol. 190, 457–1469. https://doi.org/10.1007/s12010-019-03194-9.

Rea, G., Antonacci, A., Lambreva, M.D., Mattoo, A.K., 2018. Features of cues and processes during chloroplast-mediated retrograde signaling in the alga Chlamydomonas. Plant Sci. 272, 193–206. https://doi.org/10.1016/J.PLANTSCI.2018.04.020.

Saini, R.K., Keum, Y.S., 2018. Carotenoid extraction methods: a review of recent developments. Food Chem. 240, 90–103. https://doi.org/10.1016/J.FOODCHEM.2017.07.099.

Santos, J.P., Li, W., Keller, A.A., Slaveykova, V.I., 2024. Mercury species induce metabolic reprogramming in freshwater diatom Cyclotella meneghiniana. J. Hazard. Mater. 465, 133245 https://doi.org/10.1016/J.JHAZMAT.2023.133245.

Slaveykova, V.I., Majumdar, S., Regier, N., Li, W., Keller, A.A., 2021. Metabolomic responses of green alga chlamydomonas reinhardtii exposed to sublethal concentrations of inorganic and methylmercury. Environ. Sci. Technol. 55, 3876–3887. https://doi.org/10.1021/ACS.EST.0C08416.

Telegina, T.A., Vechtomova, Y.L., Aybush, A.V., Buglak, A.A., Kritsky, M.S., 2023. Isomerization of carotenoids in photosynthesis and metabolic adaptation. Biophys. Rev. 15, 887–906. https://doi.org/10.1007/S12551-023-01156-4, 2023 15:5.

Uragami, C., Saito, K., Yoshizawa, M., Molnár, P., Hashimoto, H., 2018. Unified analysis of optical absorption spectra of carotenoids based on a stochastic model. Arch. Biochem. Biophys. 650, 49–58. https://doi.org/10.1016/J.ABB.2018.04.021.

Vallon, O., Spalding, M.H., 2009. Amino Acid Metabolism. The Chlamydomonas Sourcebook, 3, pp. 115–158. https://doi.org/10.1016/B978-0-12-370873-1.00012-5. Vol set 2.

Veith, T., Brauns, J., Weisheit, W., Mittag, M., Büchel, C., 2009. Identification of a specific fucoxanthin-chlorophyll protein in the light harvesting complex of photosystem I in the diatom Cyclotella meneghiniana. Biochimica et Biophysica Acta (BBA) - Bioenergetics 1787, 905–912. https://doi.org/10.1016/J.BBABIO.2009.04.006.

Xiao, X., Li, W., Jin, M., Zhang, L., Qin, L., Geng, W., 2023. Responses and tolerance mechanisms of microalgae to heavy metal stress: a review. Mar. Environ. Res. 183, 105805 https://doi.org/10.1016/J.MARENVRES.2022.105805.

Yao, L., Ao, J., Jeng, M.J., Bi, J., Gao, S., Sun, G., He, Q., Zhou, Z., Zhang, Y., Sun, Y., Chang, L.B., 2019. Reactive mechanism of $Cu_2ZnSnSe_4$ thin films prepared by reactive annealing of the Cu/Zn metal layer in a snsex + se atmosphere. Crystals (Basel) 9. https://doi.org/10.3390/CRYST9010010.

Zamani-Ahmadmahmoodi, R., Malekabadi, M.B., Rahimi, R., Johari, S.A., 2020. Aquatic pollution caused by mercury, lead, and cadmium affects cell growth and pigment content of marine microalga, Nannochloropsis oculata. Environ. Monit. Assess. 192, 1–11. https://doi.org/10.1007/S10661-020-8222-5.